AIMS Biophysics

AIMS Biophysics, 13(3): 302−327.
DOI: 10.3934/biophy.2026018
Received: 15 July 2026
Revised: 17 August 2026
Accepted: 21 August 2026
Published: 27 August 2026

http://www.aimspress.com/journal/biophysics

Review

Biophysical study of the tubulin code: From lattice mechanics and detyrosination to transport sorting and disease

Mao Hinomori, Sho Ito and Tatsuya Nishino*

Faculty of Advanced Engineering, Tokyo University of Science, 6-3-1 Niijuku, Katsushika-ku, Tokyo 125-8585, Japan

* **Correspondence:** Email: tnishino@rs.tus.ac.jp; Tel: +81358761462.

Abstract: Microtubules are dynamic biophysical polymers whose function is encoded by a combinatorial regulatory framework, the "tubulin code", in which α/β-tubulin isotype composition, post-translational modifications (PTMs), and lattice conformation collectively determine effector recruitment and cellular behavior. Among these PTMs, α-tubulin detyrosination has become a particularly tractable model for biophysical investigation following the identification of its enzymatic machinery. In this review, we summarized progress across six thematic areas: Methodological advances enabling causal investigation of the tubulin code; the conceptual framework of isotype-PTM epistasis; the molecular mechanism and spatial regulation of detyrosination by the vasohibin-SVBP (VASH/SVBP) complex and MATCAP/TMCP family; microtubule lattice mechanics and plus-end dynamics; effector-mediated transport sorting; and pathophysiological consequences in neurological disease, cardiac dysfunction, and cancer. A central insight was that microtubule lattice conformation, expanded (GTP-like) versus compacted (GDP), constitutes a previously unrecognized third axis of the tubulin code. Lattice expansion enhances α-tubulin C-terminal tail (CTT) accessibility and selectively promotes VASH1/SVBP catalytic activity, mechanically gating detyrosination. This state-gated mechanism couples polymer biophysics to downstream transport selectivity, with consequences for axonal differentiation, chromosome segregation, ciliary organization, and cardiac mechanics. Neuronal axonal microtubules maintaining a GTP-like expanded lattice despite being GDP-bound further illustrates lattice conformation as an independent regulatory variable. Nevertheless, no single experimental system has demonstrated this complete causal cascade, from isotype composition through lattice mechanical state and PTM enzyme accessibility to reader recruitment, in an integrated manner. Establishing a unified reconstitution and imaging workflow to validate this cascade, and defining how its breakdown drives disease, stands as the central experimental challenge

for tubulin biophysics. Microtubules are not merely structural scaffolds but a dynamic information-processing system whose biophysical logic is only beginning to be deciphered.

Keywords: tubulin code; microtubule lattice conformation; α-tubulin detyrosination; vasohibin; post-translational modification

Abbreviations: APC: adenomatous polyposis coli; CCP: cytosolic carboxypeptidase; CNS: central nervous system; CTT: C-terminal tail; cryo-EM: cryo electron microscopy; cryo-ET: cryo electron tomography; EHT: engineered heart tissue; FRET: fluorescence resonance energy transfer; H-ABC: hypomyelination with atrophy of the basal ganglia and cerebellum; HAP1: human haploid cell line 1; HS-AFM: high-speed atomic force microscopy; IDR: intrinsically disordered region; IFT: intraflagellar transport; iPSC: induced pluripotent stem cell; MAP: microtubule-associated protein; MATCAP: microtubule-associated tyrosine carboxypeptidase; MCAK: mitotic centromere-associated kinesin; MD: molecular dynamics; MEF: mouse embryonic fibroblast; PTM: post-translational modification; RGC: retinal ganglion cell; SVBP: small vasohibin-binding protein; TCP: tubulin carboxypeptidase; TIRF: total internal reflection fluorescence; TMCP: tubulin metallocarboxypeptidase; TOG: tumor overexpressed gene; TTL: tubulin tyrosine ligase; TTLL: tubulin tyrosine ligase-like; VASH: vasohibin

1. Introduction

Microtubules are polarized biophysical polymers assembled from α/β-tubulin heterodimers that are indispensable for cell division, intracellular transport, and cell motility [1]. Their dynamic behavior is fundamentally governed by the GTPase cycle of β-tubulin: Upon incorporation into the growing lattice, GTP hydrolysis drives a conformational transition of the tubulin dimer from an expanded to a compacted state, generating mechanical strain that underlies the phenomenon of dynamic instability [2]. Beyond this intrinsic mechanochemical cycle, the functional diversity of microtubule networks is further elaborated at two levels. First, the expression of distinct α- and β-tubulin isotypes directly tunes polymer dynamics by altering growth rates and catastrophe frequencies in an isoform-dependent manner [3]. Second, a rich repertoire of post-translational modifications (PTMs) is enzymatically installed onto the exposed C-terminal tails (CTTs) of polymerized tubulin. Among these, the detyrosination of α-tubulin, catalyzed by the vasohibin–SVBP (VASH/SVBP) complex, is a pivotal mark that selectively recruits or excludes specific molecular motors and microtubule-associated proteins (MAPs), generating functionally distinct microtubule subpopulations within a regulatory framework collectively termed the "tubulin code" [4–7].

Several reviews have surveyed the tubulin code from largely genetic and biochemical perspectives, cataloguing isotype diversity and the expanding repertoire of PTMs [6–8]. In this review, we instead adopt an explicitly biophysical lens: We integrate the mechanics of the microtubule lattice, historically treated as a passive scaffold, with detyrosination enzymology to argue that lattice conformation constitutes a third, mechanically gated axis of the code. This synthesis has become possible only recently through the convergence of defined-isotype recombinant tubulin, atomic-resolution structures of the VASH/SVBP and MATCAP detyrosinases, and in situ cryo-ET of the lattice, and is elaborated in Sections 3-5. Despite these advances, fundamental mechanistic questions remain

unresolved. Moreover, how cells spatially integrate the combinatorial information encoded by multiple isotypes and overlapping PTMs to establish stereotyped tubulin code patterns, and how effector proteins decode this information with spatial precision, are not understood [6]. Furthermore, although the GTP-like expanded state of the microtubule lattice has been shown to promote VASH/SVBP-mediated detyrosination [9], the atomic-level dynamic mechanisms by which lattice conformation modulates enzymatic activity have not been directly demonstrated. Although Li et al. [10] captured continuous density corresponding to the α-tubulin CTT engaged in the VASH1 catalytic groove, this structure provides a snapshot of the enzyme-bound state. Because the CTT is intrinsically disordered and conformationally heterogeneous, static X-ray crystallographic and cryo-EM analyses have not revealed how its accessibility or interaction with the enzyme changes dynamically as the lattice transitions between expanded and compacted states. Addressing this gap has therefore required complementary MD simulations and live-cell biosensor approaches [11]. Together, these gaps highlight the need for an integrated biophysical framework connecting lattice mechanics, CTT accessibility, and the enzymatic regulation of the tubulin code.

2. The technological revolution: Methodological advances enabling causal analysis

2.1. Historical limitations, recombinant tubulin, and defined-isotype microtubules

Historically, biochemical studies of microtubules relied heavily on brain-derived tubulin preparations, which comprise heterogeneous mixtures of various isotypes and diverse post-translational modifications (PTMs). This compositional complexity precluded the isolation and functional evaluation of specific isotypes or PTMs.

Structural methods also faced significant limitations: Cryo electron microscopy (cryo-EM) and X-ray crystallography often failed to resolve the electron density of intrinsically disordered regions (IDRs), such as tubulin C-terminal tails (CTTs), thereby preventing direct visualization of dynamic enzyme–tail interactions. To overcome these constraints, a critical breakthrough was the establishment of recombinant tubulin expression and purification systems capable of generating isotypically pure microtubules. A baculovirus/insect-cell expression system combined with a "double-selection strategy", incorporating an internal His-tag into the α-subunit and a cleavable Flag-tag at the C-terminus of the β-subunit, effectively eliminated contaminating endogenous tubulin from the insect cell host, enabling production of a single defined neuronal isotype combination (α1A/βIII) together with its cryo-EM structure [12]. In parallel, a complementary tumor overexpressed gene (TOG)-affinity purification method was applied to a human embryonic kidney cell line expressing a distinct, non-neuronal isotype repertoire, yielding defined α1B/βI + βIVb microtubules and enabling the first direct in vitro comparison of dynamics between defined single-isotype combinations [3].

2.2. Defined PTM writing

Concurrent advances were achieved in characterizing the enzymatic machinery of tubulin detyrosination. Vasohibin expressed in isolation exhibits limited capacity for tubulin modification: Transfection of Vasohibin into HEK293T cells resulted in only a marginal increase in detyrosinated tubulin. In contrast, co-expression with its chaperone-like partner SVBP drove a nearly complete loss of tyrosinated α-tubulin. This robust potentiation was further corroborated in mouse embryonic

fibroblasts (MEFs), where expression of the VASH/SVBP complex induced complete detyrosination of endogenous α-tubulin [4].

2.3. Single-molecule TIRF microscopy

Single-molecule total internal reflection fluorescence (TIRF) microscopy revolutionized the tracking of individual detyrosinase molecules on microtubules, revealing enzyme translocation along the lattice and the sites of catalytic activity. These observations demonstrated that the C-terminal IDR of Vasohibin engages in dynamic interplay with its acidic N-terminal region, governing the timing of enzyme dissociation and the rate of one-dimensional diffusion along the lattice [13]. At the population level, VASH1 acts broadly across the microtubule network, whereas VASH2 generates discrete, patch-like detyrosination patterns. This dichotomy primarily reflects the substantially longer microtubule residence time of VASH2 relative to VASH1; in both enzymes, interplay between the N-terminal and C-terminal IDRs provides the precise kinetic control that sets this residence time [13]. Furthermore, single-molecule imaging using an antibody-based biosensor confirmed that VASH1/SVBP activity is specifically enhanced on microtubules adopting a GTP-mimicking, expanded lattice conformation [9], establishing that the lattice structural state functions as an allosteric switch for the detyrosinase.

2.4. Cryo-EM/ET and structural analysis

The structural basis for the preferential activity of VASH1/SVBP toward polymerized tubulin was elucidated via cryo-EM. The interface between VASH1 and two adjacent α-tubulin molecules spanning neighboring protofilaments is geometrically incompatible with free αβ-tubulin dimers and can be established only on the assembled lattice; disruption of these lattice-specific contacts selectively abolishes detyrosination of microtubule polymers while leaving activity toward soluble tubulin largely intact [10]. Building upon this framework, the integration of cryo-ET with coarse-grained computational modeling, supported by atomistic simulations, revealed that protofilaments at the microtubule plus-end form an ensemble of multiple conformational states, with GTP/GDP-dependent mechanical selection (conformational selection) governing the transition between growth and catastrophe [14].

2.5. Molecular dynamics simulation

MD simulations indicated that the α-tubulin CTT does not fluctuate freely but instead forms transient, numerous contacts with the globular bodies of both α- and β-tubulin within the lattice, adopting a "stored" conformation. Contacts involving the distal portion of the CTT were more frequent under GDP/compacted conditions and reduced under GTP-like/expanded conditions, consistent with greater CTT accessibility in the expanded lattice. Complementary single-molecule biosensor imaging in living cells supports this difference in accessibility; however, these biosensor data indicate a correlation and do not by themselves establish that increased accessibility is the direct cause of enhanced VASH1/SVBP catalysis, leaving open the possibility of additional conformational effects on productive enzyme engagement [11].

2.6. Integration and remaining challenges

Collectively, the methodological advances described in this section, recombinant tubulin of defined composition, single-molecule TIRF microscopy, cryo-EM/ET, and MD simulation, have transformed microtubule biology from a correlative to a causal discipline. Nevertheless, a unified workflow capable of applying TIRF-based kinetic measurements, cryo-EM structural analysis, and quantitative kinetic modeling to an identical, defined sample in parallel remains to be established. More broadly, the persistent epistemological gap between computational prediction and experimental validation has been identified as a central challenge in protein biophysics, underscoring the need for genuinely integrated approaches [15]. Bridging this gap will likely require multiscale strategies that connect atomistic MD, typically limited to trajectories of nanoseconds to a few microseconds, with the millisecond-to-second timescales accessible to TIRF-based single-molecule and bulk enzymatic assays. Coarse-grained MD simulations and Markov state models, which compress atomistic trajectories into a small number of long-lived conformational states and their inter-state transition kinetics, offer one computational route to this extrapolation, while high-speed atomic force microscopy (HS-AFM), capable of resolving CTT and lattice dynamics with sub-second temporal and sub-nanometer spatial resolution, offers a complementary experimental bridge. Neither approach has been applied to the VASH/SVBP-microtubule system, and their integration constitutes an important methodological frontier for the field.

3. The tubulin code

3.1. Conceptual definition

The “tubulin code” is a conceptual framework in which the functional identity of a microtubule is determined by the combination of α/β-tubulin isotypes expressed by the cell and the chemically diverse array of post-translational modifications (PTMs) deposited on their surfaces [6,7]. PTMs are added and removed by dedicated enzymatic machineries designated “writers” and “erasers”, respectively, while a distinct class of proteins termed “readers” decode the resulting modification patterns through selective binding to or dissociation from the microtubule lattice [8]. Despite these advances, the fundamental mechanisms by which cells write and read the tubulin code remain largely unresolved [6].

3.2. Isotype composition tunes lattice structure and dynamics

Microtubules reconstituted from the α1B/βI + βIVb isotype combination, purified from a human embryonic kidney-derived (tsA201) cell line, display faster elongation rates and lower catastrophe frequencies relative to brain-derived heterogeneous tubulin [3]. Titrating in an increasing proportion of the recombinant neuron-specific α1A/βIII heterodimer, produced separately using a baculovirus-insect cell (Sf9) expression system, progressively decreased the elongation rate and elevated catastrophe frequency, providing direct evidence that isotype composition actively tunes microtubule dynamics [3]. These data show that isotype composition directly alters microtubule growth and catastrophe behavior and is accompanied by differences in plus-end taper and tubulin curvature [3]. The molecular sequence features responsible for these changes were not directly resolved in that study.

The structural basis of the GTP hydrolysis-driven lattice transition (expanded → compacted state) is discussed in detail in Section 5; however, the rate of this transition may be isotype-dependent, providing a potential molecular explanation for the observed differences in catastrophe frequency [2,3].

3.3. PTMs regulate effector recruitment

Decoding of the tubulin code is executed by effector proteins that recognize PTM patterns on the microtubule surface. A key principle established by quantitative in vitro reconstitution is that PTMs, including detyrosination, do not directly alter the intrinsic dynamics of the microtubule polymer; rather, they function as docking signals that selectively recruit or exclude specific effector molecules [16]. For example, +TIP proteins harboring CAP-Gly domains, such as CLIP-170 and $p150^{Glued}$, fine-tune their association with microtubule plus-ends in a tyrosination-dependent manner [16]. The most spatially precise demonstration of code-dependent transport selectivity comes from the intraflagellar transport (IFT) system: VashL-knockout *Chlamydomonas reinhardtii* mutants, in which the tyrosination/detyrosination balance is disrupted and exhibit frequent IFT train stalling and impaired ciliary elongation; direct measurement revealed that anterograde and retrograde trains possess distinct affinities for A- and B-tubules that depend on their tyrosination status [17].

Detyrosination is one component of a broader PTM code. Work from Janke and colleagues established the tubulin tyrosine ligase-like (TTLL) family as a major class of tubulin-modifying enzymes; a TTLL1-containing complex catalyzes tubulin polyglutamylation [18]. Polyglutamylation can tune effector activity in a graded manner: Longer glutamate side chains promote spastin-dependent microtubule severing in cells and in vitro [19]. Moreover, TTLL1 and TTLL7 preferentially generate polyglutamylation on α- and β-tubulin, respectively, and these subunit-specific modification patterns have distinct effects on axonal transport and neurodegeneration [20]. These findings provide an independent experimental demonstration that the identity, location, and extent of a tubulin PTM can encode distinct functional outputs, complementing the tyrosination/detyrosination system emphasized here.

3.4. Isotype × PTM epistasis and the lattice as a third axis

Integrating the physical consequences of isotype diversity with the chemical selectivity conferred by PTMs reveals that the tubulin code functions not through the independent action of each layer, but through synergistic or antagonistic epistatic interactions between them [6,8]. Defined-isotype microtubules exhibit distinct dynamic and structural properties, including differences in growth, catastrophe behavior, plus-end taper, and tubulin curvature [3]. This raises the possibility that the many isotype, PTM combinations that remain experimentally uncharacterized are coupled to structural changes arising from GTP hydrolysis-driven lattice dynamics. Critically, lattice expansion has been shown to promote VASH1/SVBP detyrosinase activity [9] and to enhance enzymatic accessibility to the α-tubulin CTT [11], suggesting that lattice structural state itself constitutes a previously unrecognized axis of the tubulin code (Figure 1). Disease models further suggest coupling between the isotype and PTM axes. In a TUBB4A A302T model of H-ABC tubulinopathy, white-matter regions showed increased α-tubulin detyrosination and acetylation together with altered β-tubulin phosphorylation, consistent with a shift toward a more stable microtubule state [21]. Because detyrosinase kinetics and lattice conformation were not measured directly, it remains unresolved

whether the β-tubulin mutation changes α-tubulin detyrosination through altered lattice structure, increased microtubule lifetime, or changes in PTM-enzyme access. This disease context therefore provides a particularly relevant system in which to test the proposed isotype–lattice–PTM coupling.

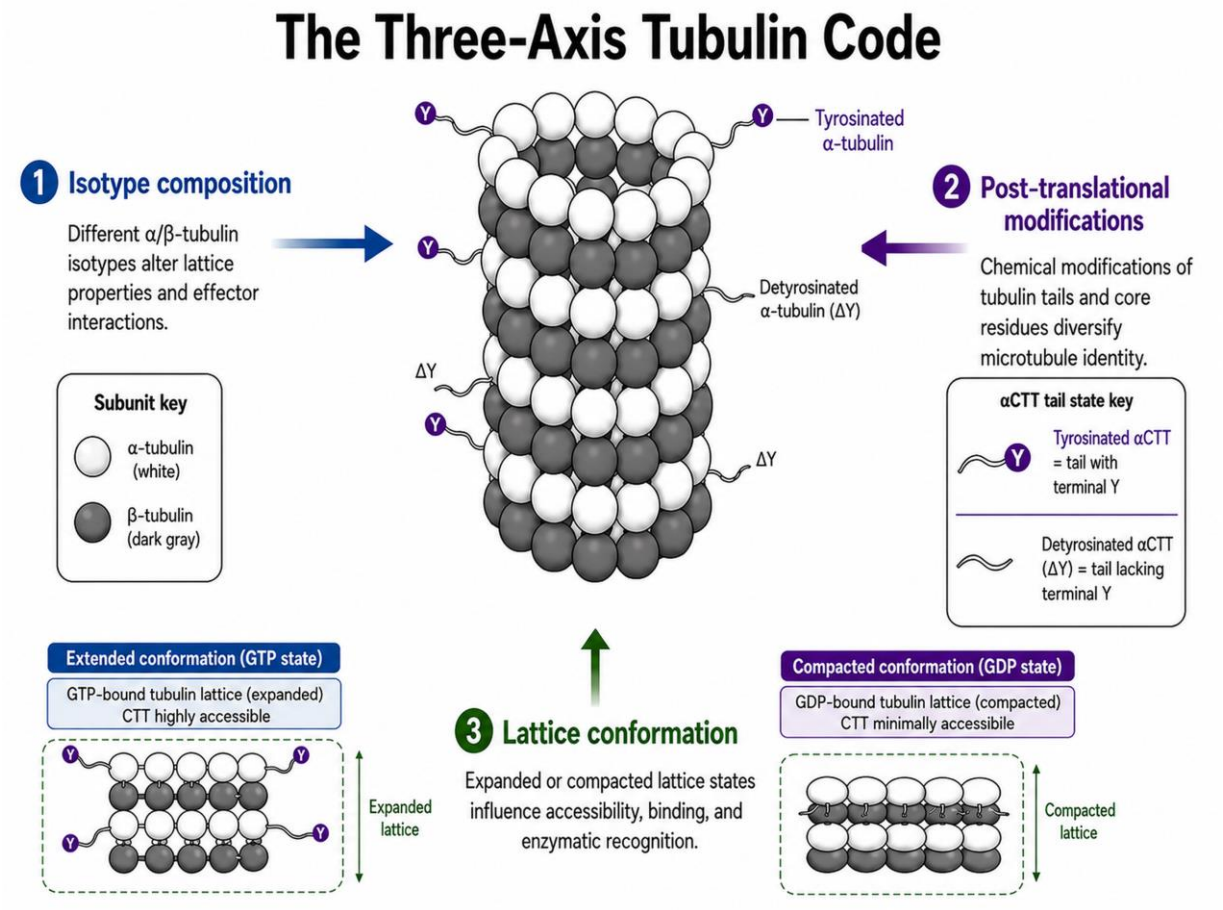

Figure 1. The tubulin code as a three-axis combinatorial system.

The functional identity of a microtubule is determined by three interacting regulatory layers. (1) Isotype composition: Different α/β-tubulin isotypes alter intrinsic lattice properties and effector interactions (Section 3). (2) Post-translational modifications: Chemical modifications of the α-tubulin C-terminal tail (CTT) and core residues diversify microtubule identity; tyrosinated (Y) and detyrosinated (ΔY) α-tubulin subunits are indicated on the lattice model (Section 4). (3) Lattice conformation: Expanded versus compacted lattice states influence CTT accessibility, enzyme binding, and enzymatic recognition, constituting the third, previously unrecognized axis of the tubulin code proposed in this review (Section 5). α-Tubulin subunits are shown in white and β-tubulin subunits in dark gray; the αCTT tail-state key at right distinguishes tyrosinated (Y) from detyrosinated (ΔY) tails. In the lattice-conformation insets, the αCTT is depicted as a less-accessible, lattice-associated ("stored") conformational ensemble in the compacted state and as a more accessible ensemble in the expanded state. These cartoons represent relative accessibility rather than an absolute hidden/exposed switch [11].

3.5. Remaining open questions

A central unresolved question concerns the quantitative epistasis between the isotype backbone and PTM writing efficiency: How do isotype-dependent differences in sequence influence the ability of writers and erasers to amplify or attenuate specific modifications? Comprehensive quantitative datasets addressing this question are not available [8]. Furthermore, no researcher has demonstrated the complete causal cascade "isotype → lattice mechanical state → PTM enzyme accessibility → reader recruitment" in a single integrated experimental system; each link in this chain has been established independently, and their concatenation remains inferential [6,9].

4. α-tubulin detyrosination

4.1. Historical context and identification of VASH/SVBP as TCP

Vasohibin (VASH) was originally identified in the context of angiogenesis research. In 2004, Watanabe and colleagues, through a comprehensive screen for VEGF-inducible genes, identified an uncharacterized gene, KIAA1036, and found that its recombinant protein selectively inhibited the migration, proliferation, and tube formation of vascular endothelial cells. Because this protein was induced by VEGF while suppressing angiogenesis, it was named "vasohibin", reflecting its proposed role as an endothelium-derived negative feedback regulator of angiogenesis [22]. Its homolog VASH2 was subsequently isolated, establishing the concept that the vasohibin family constitutes a genetically programmed angiogenesis-regulatory system within endothelial cells [23]. This role as an angiogenesis inhibitor remained the sole known function of VASH for over a decade.

The existence of an α-tubulin detyrosinating enzyme (tubulin carboxypeptidase, TCP) had been postulated since the 1970s, but its molecular identity remained unknown for decades. Aillaud et al. [4] employed chemical proteomics using an irreversible inhibitor (epoY), while Nieuwenhuis et al. [5] independently conducted a genome-wide genetic screen in human haploid (HAP1) cells; both approaches converged on the identification of a complex between vasohibin-1 (VASH1), its homolog VASH2, and the small vasohibin-binding protein (SVBP) as the long-sought TCP. This revealed that VASH, previously characterized solely as a secreted angiogenesis-regulatory protein, performs a distinct cellular function as a tubulin-detyrosinating enzyme [24].

4.2. Structural basis and catalytic mechanism

Following the identification of VASH as an α-tubulin detyrosinase, high-resolution crystal structures were rapidly determined: VASH1/SVBP [25] and VASH2/SVBP complexes [26]. How the enzyme engages the microtubule lattice was determined by the cryo-EM structure capturing VASH1/SVBP docked onto the microtubule lattice [10] (Figure 2A). The catalytic site of VASH1 is a cysteine protease bearing a non-canonical Cys-His-Leu catalytic triad. The corresponding VASH2 triad has been reported differently across structural studies: Wang et al. [26] described a conserved Cys-His-Leu triad shared with VASH1, whereas Zhou et al. [27] reported a distinct non-canonical Cys-His-Ser architecture specific to VASH2; reconciling this discrepancy will require direct side-by-side structural comparison. Structural analysis further showed that the C-terminal tyrosine of α-tubulin is accommodated within a hydrophobic pocket on the VASH surface, while the core domain engages the

microtubule lattice through electrostatic interactions.

4.3. SVBP as chaperone and the heterotetrameric complex

VASH does not function as an enzyme in isolation. Heteromeric association with the small vasohibin-binding protein SVBP was shown to be indispensable for catalytic activity [4]. Zhou et al. [27] further demonstrated, at the structural level, that VASH2, intrinsically unstable on its own within cells, forms a highly dynamic, positively charged groove spanning its catalytic pocket through the α1 and α2 helices, and that SVBP acts as a chaperone-like partner by extensively engaging and stabilizing these helices.

VASH/SVBP complexes are not restricted to heterodimers; they can also assemble into domain-swapped heterotetramers. In this arrangement, two heterodimers cross over one another, with a variable arm region extending from one VASH1 molecule exchanging with the core and arm of the partner heterodimer, thereby forming a robust heterotetrameric assembly [28].

4.4. Lattice conformation-dependent activity and CTT accessibility

VASH1/SVBP associates with microtubules irrespective of whether the tubulin subunits adopt a compacted or expanded conformation. However, its detyrosination activity is markedly enhanced on expanded lattices, including GMPCPP microtubules and Taxol-stabilized GDP microtubules. These findings indicate that lattice conformation regulates VASH1/SVBP-mediated detyrosination primarily at the level of catalytic activity rather than through selective recruitment of the enzyme to the microtubule [9].

The C-terminal tails (CTTs) of α- and β-tubulin were conventionally thought to extend freely from the microtubule surface. However, Hotta et al. [11] developed biosensors specific for the α-tubulin CTT and demonstrated that the αCTT is less accessible along much of the microtubule lattice than previously assumed. Its accessibility increases under conditions that promote lattice expansion, including Taxol treatment, binding of lattice-expanding microtubule-associated proteins, and expression of hydrolysis-deficient tubulin. Molecular dynamics (MD) simulations further indicated that the αCTT forms numerous transient interactions with the globular surfaces of α- and β-tubulin and that the frequency and distribution of these interactions are modulated by nucleotide- and effector-dependent changes in lattice conformation. Thus, lattice expansion shifts the αCTT toward a more accessible conformational ensemble that facilitates engagement by VASH1/SVBP and enhances detyrosination. Notably, this nucleotide–conformation link is not fully direct: When the same probes were applied to microtubules reconstituted in vitro in the absence of MAPs, GMPCPP- and GDP-microtubules showed no significant difference in steady-state αCTT accessibility, indicating that nucleotide state alone is insufficient to gate CTT exposure and that MAP-mediated lattice remodeling is the more proximal determinant [11]. This discrepancy, explicitly noted by the original authors, tempers the strength of the inference that lattice conformation directly and universally gates detyrosinase accessibility, and underscores the need for future reconstitution systems that incorporate physiological MAP occupancy to resolve this apparent contradiction.

Studies have extended this lattice-state-dependent regulatory framework to MATCAP1 while revealing a mechanistically distinct mode of regulation. In contrast to VASH1/SVBP, MATCAP (also termed MATCAP1 in later literature) preferentially binds to microtubules containing tubulin subunits

in an expanded conformation. Expansion induced by inhibition of β-tubulin GTP hydrolysis, Taxol treatment, or kinesin-1 stepping enhances MATCAP binding and enzymatic activity. Once bound, MATCAP1 exhibits a long residence time on the microtubule lattice and sequentially removes the C-terminal tyrosine and the penultimate glutamate residue of α-tubulin to generate ΔY-tubulin (detyrosinated α-tubulin) and Δ2-tubulin (also denoted ΔC2-tubulin in some literature, e.g., Yue et al. [29]; lacking both C-terminal tyrosine and penultimate glutamate), respectively [29]. These findings indicate that lattice conformation can regulate different detyrosinating enzymes at distinct mechanistic steps: Predominantly catalytic activity in the case of VASH1/SVBP, but lattice recruitment and catalytic activity in the case of MATCAP.

A complementary observation comes from in vivo studies of microtubule lattice organization. High-resolution (2.7 Å) in situ structural analysis of microtubules within neuronal axons revealed that, despite being fully GDP-bound, the lattice maintains an expanded conformation resembling the GTP state. This finding demonstrates that lattice conformation is not determined solely by the nucleotide state of β-tubulin and that lattice expansion can be acquired and maintained as a cell-state-dependent structural feature during neuronal differentiation and axon formation [30]. Thus, the expanded lattice may function as an independent regulatory variable that influences CTT accessibility and the enzymatic writing of tubulin post-translational modifications.

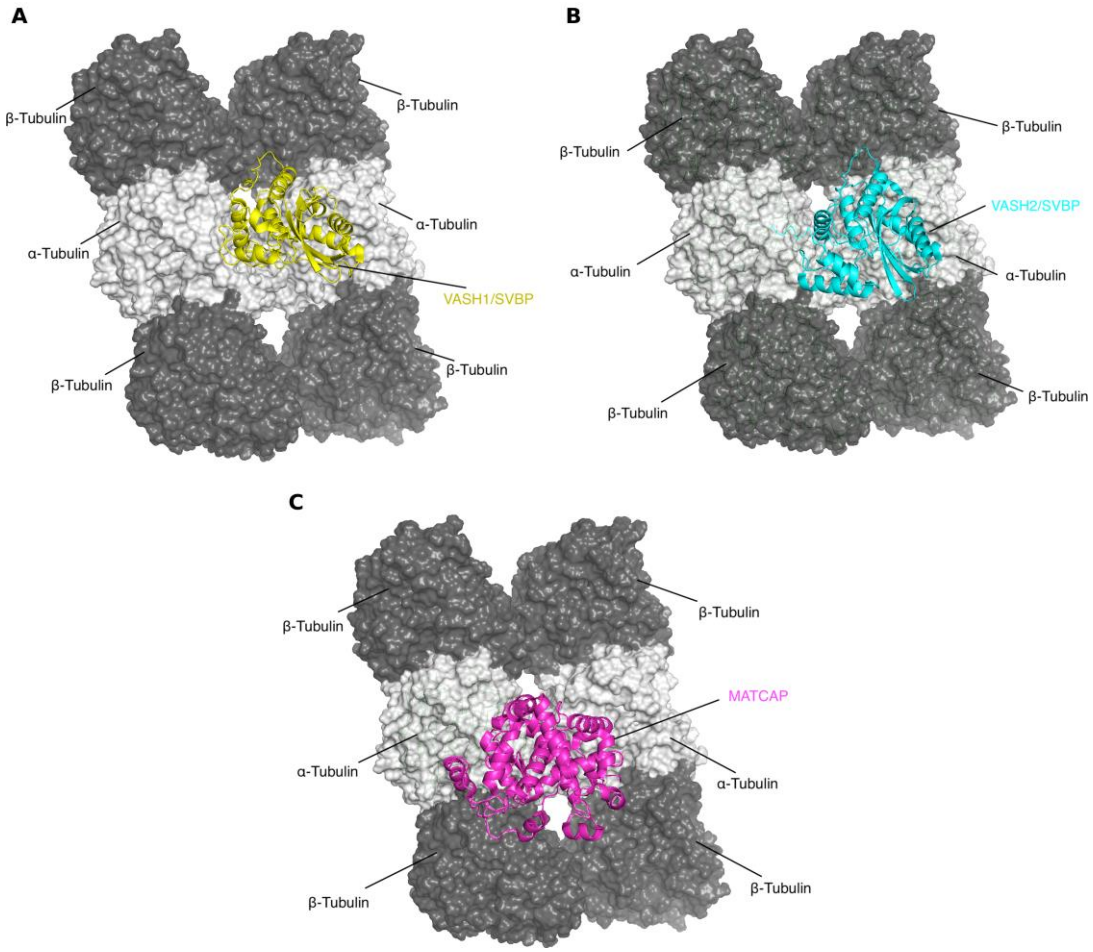

Figure 2. Distinct structural modes of microtubule recognition by VASH1/SVBP, VASH2/SVBP, and MATCAP.

(A) Composite structural model of human VASH1/SVBP bound to the microtubule lattice. The VASH1/SVBP complex was extracted from the cryo-EM structure of microtubule-bound VASH1/SVBP (PDB ID: 6WSL) and superposed onto the common microtubule lattice framework derived from the GMPCPP-stabilized VASH2/SVBP–microtubule structure (PDB ID: 7ZCW) by alignment of the corresponding α-tubulin subunits. VASH1/SVBP is shown as a yellow cartoon representation. The model illustrates the inter-protofilament binding mode of VASH1/SVBP, in which the enzyme contacts α-tubulin subunits from two neighboring protofilaments. Note that 6WSL was solved using 14-protofilament GMPCPP-stabilized microtubules; the composite model facilitates direct comparison of binding geometries on a common 13-protofilament microtubule reference frame.

(B) Cryo-EM structure of human VASH2/SVBP bound to the GMPCPP-stabilized microtubule lattice (PDB ID: 7ZCW). VASH2/SVBP is shown as a cyan cartoon representation. Similar to VASH1/SVBP, the complex engages α-tubulin subunits across adjacent protofilaments, although VASH2/SVBP adopts a distinct orientation on the lattice.

(C) Cryo-EM structure of MATCAP bound to the microtubule lattice (PDB ID: 7Z6S). MATCAP is shown as a magenta cartoon representation. In contrast to the inter-protofilament recognition mode of the VASH/SVBP complexes, MATCAP interacts predominantly with longitudinally adjacent tubulin subunits within a single protofilament, illustrating a distinct intra-protofilament binding mode.

For all panels, the microtubule lattice is displayed as a surface representation in the same orientation. α-Tubulin subunits are colored white and β-tubulin subunits are dark gray. The common lattice representation facilitates direct comparison of the distinct microtubule-binding geometries adopted by the three detyrosinating enzyme systems. Structural models were prepared and rendered using PyMOL.

4.5. VASH1 vs. VASH2: global versus local detyrosination profiles

VASH1 and VASH2 exhibit distinct spatial profiles of detyrosination: VASH1/SVBP generates broad, global detyrosination across the microtubule network, whereas VASH2/SVBP produces localized, patch-like modifications [13] (Figure 2B; Figure 3). Regarding this lattice-conformation dependence, two contemporaneous papers offer differing explanatory frameworks whose relationship remains incompletely resolved. Yue et al. [9] reported that while the binding of VASH1/SVBP to microtubules does not differ between GTP-mimetic and GDP states, catalytic activity, the efficiency of the detyrosination reaction, is markedly higher on the GTP-mimetic, expanded lattice. Tang et al. [31], by contrast, used single-molecule tracking to show that VASH engages with nearly all microtubules through stochastic, short-lived interactions, and proposed a model in which the emergence of detyrosination subsets can be explained by a positive feedback loop between stochastic enzyme engagement and microtubule stability, without invoking lattice conformation as an explicit variable. Whether these two models are genuinely in conflict, or whether the conformation-dependent activation mechanism reported by Yue et al. [9] provides the underlying molecular basis the feedback loop proposed by Tang et al. [31], remains an important open question that has not yet been experimentally resolved. One possible reconciliation, offered here as a testable hypothesis rather than an established mechanism, is that the two models describe sequential rather than mutually exclusive steps. In this scenario, transient lattice expansion, induced locally by MAP or motor binding or generated at sites of lattice repair (Section 5.4), would act as the initiating event that renders a stochastic VASH1/SVBP-microtubule encounter catalytically productive, consistent with Yue et al. [9];

the resulting local detyrosination mark would then favor further recruitment of expander MAPs and motors, reinforcing lattice expansion and enzyme engagement in a self-amplifying loop consistent with the stability-dependent feedback model of Tang et al. [31]. Distinguishing this integrated model from either model in isolation will require simultaneous, correlated measurement of lattice conformation, enzyme engagement, and detyrosination state on the same microtubule over time, a capability that does not yet exist (Section 5.6).

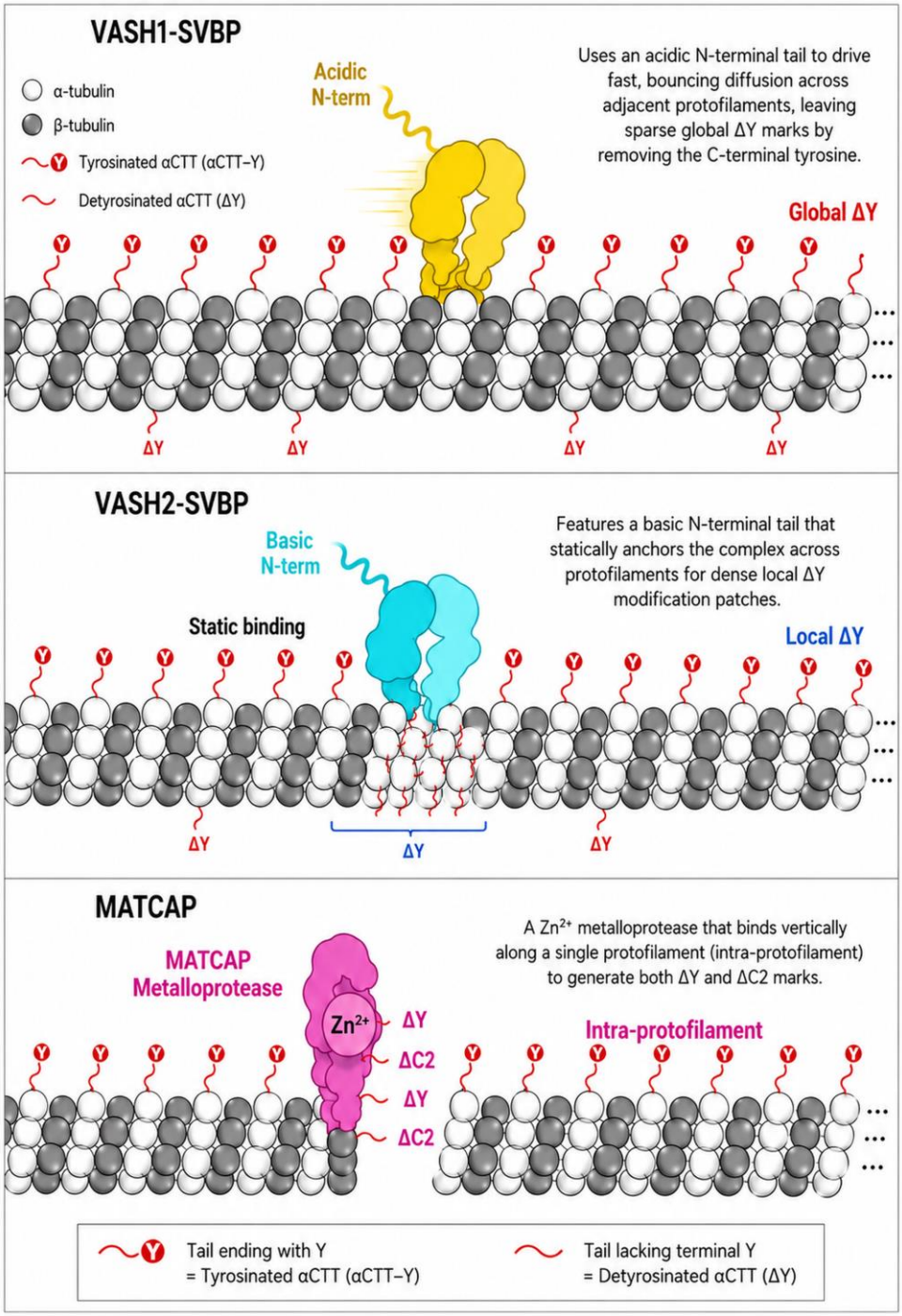

Figure 3. Distinct kinetic and spatial mechanisms generate global, local, and dual-site detyrosination patterns.

VASH1/SVBP: An acidic N-terminal intrinsically disordered region (IDR) promotes fast, bouncing diffusion across adjacent protofilaments, generating sparse, broadly distributed (global) ΔY marks by removal of the C-terminal tyrosine (Section 2.3; Section 4.5) [13].

VASH2/SVBP: A longer microtubule residence time conferred by its N-terminal IDR statically anchors the complex, producing dense, spatially confined (local) ΔY patches (Section 2.3; Section 4.5) [13].

MATCAP: A Zn^{2+}-dependent metalloprotease that engages tubulin subunits longitudinally within a single protofilament (intra-protofilament recognition; Figure 2C), sequentially removing the C-terminal tyrosine and the penultimate glutamate to generate ΔY- and Δ2-tubulin (Section 4.6) [29,32,33]. Together, the three enzyme systems illustrate how distinct kinetic behaviors (diffusive vs. static binding) and distinct lattice-recognition geometries (inter- vs. intra-protofilament) translate into markedly different spatial patterns of the detyrosination mark. Subunit and tail-state keys are shown at the bottom.

4.6. MATCAP/TMCP family: a second detyrosination system

The persistence of residual detyrosination activity in cells lacking VASH/SVBP had long suggested the existence of an unidentified enzyme. Landskron et al. [32] identified this enzyme through a genetic screen and named it MATCAP (microtubule-associated tyrosine carboxypeptidase) (Figure 2C; Figure 3). This enzyme was shown to play an important role in regulating microtubule dynamics during neurogenesis and brain development, with broader relevance to behavior, and detyrosination status has separately been associated with mitotic fidelity; MATCAP is capable of acting without requiring a binding partner analogous to SVBP. Nicot et al. [33] subsequently classified MATCAP (designated TMCP1) together with its paralog KIAA0895 (TMCP2) within a common TMCP (tubulin metallocarboxypeptidase) family. Assays for measuring the activity of these enzymes had historically relied heavily on antibody-based detection, making it difficult to determine kinetic parameters such as Michaelis–Menten constants. Simon et al. [34] developed a real-time FRET-based assay that now enables quantitative measurement of activity, although it still relies on peptide substrates and therefore remains limited in evaluating inhibitors that target lattice-specific enzyme–substrate interactions.

4.7. TTL and re-tyrosination: completing the cycle

While VASH/SVBP and MATCAP target polymerized microtubule lattices, the enzyme responsible for re-tyrosination, tubulin tyrosine ligase (TTL), binds free, soluble αβ-tubulin dimers released upon microtubule depolymerization, thereby resetting and renewing the modification state of the tubulin pool [35]. Pietsch et al. [36] demonstrated that chronic AAV-mediated TTL overexpression dramatically reduced the abnormally elevated levels of detyrosinated microtubules (dTyr-MTs) and restored normal tyrosination levels in a hypertrophic cardiomyopathy mouse model and in patient-derived induced pluripotent stem cell (iPSC) cardiomyocytes. In a complementary engineered heart tissue (EHT) system, CRISPR/Cas9-mediated knockout of SVBP, rather than TTL overexpression, was used to chronically activate tubulin tyrosination: SVBP-deficient EHTs displayed improved force development and faster relaxation, whereas TTL-knockout EHTs showed the opposite phenotype, together confirming that the detyrosination/re-tyrosination cycle bidirectionally regulates cardiac

mechanical function.

4.8. α-tubulin ΔY → Δ2 processing cascade

The α-tubulin C-terminal glutamate residue exposed by detyrosination is further removed by the cytosolic carboxypeptidase family, generating Δ2-tubulin. Δ2-tubulin cannot be re-tyrosinated by TTL and accumulates on stable microtubule subpopulations as an irreversibly modified state. Beyond this Tyr/Glu removal cascade, other TMCP family members additionally possess deglutamylase activity, a mechanistically distinct process that removes post-translationally added polyglutamate side chains rather than genetically encoded C-terminal residues [33], indicating that tubulin tail processing by the TMCP family extends beyond ΔY→Δ2 generation to encompass polyglutamylation removal as well. The spatiotemporal regulation of this cascade remains unresolved and constitutes an important direction for future research.

5. Microtubule structure, mechanics, and end-state dynamics

5.1. Lattice structure and GTP hydrolysis-driven conformational transitions

Microtubules are hollow cylindrical polymers assembled from α/β-tubulin heterodimers that polymerize head-to-tail to form protofilaments, which associate laterally to generate the tubular wall. The conformation of tubulin is dictated by the identity of the bound nucleotide. Free GTP-bound tubulin adopts a curved conformation in solution, but upon incorporation at the growing plus-end, it is constrained into a straight configuration. Alushin et al. [2] resolved the structural consequences of GTP hydrolysis within the assembled lattice at unprecedented resolution using cryo-EM and Rosetta modeling. Conversion from a GTP-state to a GDP-state lattice is accompanied by longitudinal compaction of the tubulin dimer; release of inorganic phosphate generates a cavity at the E-site that drives inward contraction of β-tubulin, storing mechanical strain that disfavors the straight protofilament conformation and propagates a destabilizing stress throughout the lattice. Taxol alleviates this strain by binding allosterically to β-tubulin and stabilizing a conformation resembling the GMPCPP-bound (GTP-mimetic) state, thereby suppressing the structural transitions associated with hydrolysis.

Lattice conformation is not exclusively governed by the intrinsic GTPase cycle. Allosteric effectors, MAPs, motor proteins, and pharmacological agents can independently trigger conformational switching upon engagement with the lattice surface. Locally induced conformational changes propagate beyond the immediate binding site, transmitting structural information deep into the assembled lattice. The physical mechanism underlying this cooperative propagation remains incompletely characterized, and there is emerging evidence that the susceptibility to conformational switching (i.e., lattice plasticity) differs among tubulin isotypes in their response to Taxol and MAP binding, although the isotype-specific determinants of this plasticity have not been systematically resolved [37].

5.2. Plus-end dynamics: from single states to conformational ensembles

Building on structural analyses of the GTP-cap model of dynamic instability by Alushin et al. [2]

and others, integrated cryo-ET and coarse-grained modeling, supported by atomistic simulations, has revealed that protofilaments at the growing plus-end do not behave as independent entities but instead form transient lateral clusters with neighboring protofilaments. Whether a microtubule grows or catastrophizes is determined by a process of conformational selection: The nucleotide state of the terminal tubulin dictates which type of cluster assembles at the end. GTP-bound protofilaments are flexible and tend to form short-lived but stable clusters that favor continued elongation, whereas GDP-bound protofilaments are rigid and form heterogeneously elongated clusters in which internal pressure accumulates until structural failure triggers catastrophe [14].

Complementary to this structural perspective, Cleary et al. [38] used interference reflection microscopy (IRM) to quantify growth-rate fluctuations with high precision as a function of GTP hydrolysis status. Under conditions that suppress hydrolysis, microtubules elongate with remarkably low variance. This stabilization implies that hydrolysis proceeds in close proximity to the growing tip, such that GDP-bound tubulin is transiently exposed at the plus-end even during active growth, and it is this transient GDP exposure that is the primary source of growth-rate fluctuations. These findings support models in which longitudinal interactions are strong and the GTP-cap is thin rather than a thick protective buffer.

5.3. The GTP cap: evidence from mosaic microtubules

Direct characterization of the GTP-cap has historically been complicated by the fact that available tools, non-hydrolyzable GTP analogs such as GMPCPP, and hydrolysis-deficient tubulin variants, perturb lattice biochemistry and geometry in ways that confound interpretation. Estévez-Gallego et al. [39] circumvented this limitation by designing “mosaic microtubules” in which two variants were mixed at an optimized ratio to faithfully mimic the GTP-cap. Cryo-EM structural analysis of this system revealed that the principal structural feature distinguishing GTP-state from GDP-state tubulin within the lattice is longitudinal expansion of the lattice spacing rather than protofilament twist. In a parallel approach, Zhou et al. [40] resolved the structural trajectory of tubulin polymerization by cryo-EM, showing that soluble GDP- and GMPCPP-bound tubulin dimers are both substantially curved and that GTP binding primarily increases conformational flexibility and favors productive lateral-contact formation; it is the progressive closure of these lateral contacts during assembly, rather than GTP binding, that drives the transition to the straightened, polymerized conformation.

Integrating these findings, free GTP-bound tubulin dimers are curved prior to polymerization; the essential contribution of GTP is to lower the energetic barrier for lateral contact formation. As lateral bonds close sequentially, the curved heterodimers are mechanically straightened. These insights extend the classical GTP-cap concept beyond a purely biochemical definition: The plus-end must be understood as a physical entity whose behavior is shaped not only by nucleotide identity, but also by the balance of longitudinal and lateral interaction energies and by the conformational ensemble of the terminal protofilaments [1,14].

5.4. Lattice defects, repair, and a hypothesis linking detyrosination

The microtubule lattice, once viewed as a geometrically uniform cylinder, is a structurally heterogeneous assembly. Stochastic variability in GTP hydrolysis timing and mechanical stresses imposed on the lattice generate local sites of structural irregularity, lattice defects, characterized by

variations in protofilament number or by discontinuities in the tubular wall [1]. Incorporation of fresh GTP-bound tubulin at these defect sites can restore lattice continuity, and the resulting locally GTP-state domains may function as kinetic barriers against depolymerization, constituting a self-repair mechanism that extends the microtubule lifetime.

In the context of Section 4, where Yue et al. [9] demonstrated that VASH/SVBP preferentially acts on expanded, GTP-mimetic lattice conformations, an intriguing, as-yet experimentally untested hypothesis emerges: We speculate that VASH/SVBP may preferentially recognize and detyrosinate GTP-state tubulin incorporated at lattice repair sites, thereby linking the local structural state of the lattice to the spatial patterning of detyrosination. This hypothesis is not supported by direct experimental evidence; its verification would require correlated imaging of lattice-repair events and detyrosination activity at single-molecule resolution. Experimental verification of this hypothesis represents an important direction for future work.

5.5. In vivo lattice states: correspondence and divergence from in vitro data

The lattice conformational transitions extensively characterized in vitro had not been directly verified in the cellular context until recently. Cryo-ET analysis of microtubules decorated with StableMARK, a fluorescent probe that selectively binds stable microtubule subpopulations within living cells, demonstrated that StableMARK-positive microtubules predominantly adopt an expanded lattice conformation, establishing a correlation between the stable, MAP-decorated microtubule population and lattice expansion in vivo [41].

A particularly striking finding comes from the in situ structural analysis of axonal microtubules. Zehr et al. [30] applied cryo-EM to microtubules within axons of cortical neurons differentiated from human iPSCs, achieving 2.7 Å resolution. Despite being fully GDP-bound, these microtubules maintained a lattice expansion characteristic of the GTP state, a conformation that was absent in undifferentiated iPSCs, whose microtubules adopted the compacted GDP-state lattice. This finding demonstrates that lattice expansion is not a passive consequence of nucleotide binding state but an actively regulated cellular feature acquired during the differentiation program that produces mature neurons with stable axons. It further challenges the in vitro-derived generalization that GDP-bound lattices are invariably compacted, highlighting the need to critically evaluate the in vivo relevance of all in vitro structural observations. The possibility that lattice conformation encodes a physical memory of differentiation state is revisited in Section 6. The molecular basis for this actively maintained expansion remains speculative. A straightforward hypothesis would invoke stabilization by axon-enriched MAPs; however, the principal axon-enriched MAP, tau, has been reported to recognize or induce a compacted rather than an expanded lattice in vitro [11], while MAP2, an expander-lattice-associated MAP in some contexts, is largely somatodendritic and excluded from mature axons. This apparent paradox, an axon-specific compacting MAP coexisting with an axon-specific expanded lattice, underscores how incompletely the maintenance mechanism is understood and argues against a simple compactor/expander-MAP explanation. More plausible candidate mechanisms include local, persistent occupancy by expander MAPs or motors characterized in non-neuronal contexts, such as kinesin-1, MAP7, or CAMSAP family proteins [11]; continuous mechanical loading from axonal transport and cytoskeletal cross-linking; and isotype-specific differences in lattice plasticity, since the neuron-enriched βIII-tubulin isotype has been reported to respond differently to expansion-inducing ligands and MAPs than other β-tubulin isotypes [37]. Directly testing these candidate mechanisms in axonal

preparations is an important priority, raised again in Section 5.6.

5.6. Open questions and next experimental steps

Three open questions emerge from the structural and mechanical framework developed in this section. First, the ensemble of plus-end states defined in vitro, protofilament clustering, transient GDP exposure, and GTP-cap dimensions, has not been directly characterized under the biochemical conditions prevailing within the cell, where MAPs, mixed isotype composition, and molecular crowding may substantially alter these properties. Second, the spatial relationship between lattice defect and repair sites and the preferred substrates of detyrosination enzymes remains unknown; establishing whether locally GTP-state domains at repair sites function as detyrosination hotspots would directly address the unresolved mechanistic competition between the models proposed by Yue et al. [9] and Tang et al. [31] (Section 4). Third, the quantitative relationship between isotype composition (Section 3) and lattice conformation or end-state dynamics has not been resolved; systematic comparison of GTP-cap dimensions and catastrophe thresholds across defined single-isotype microtubules using correlated cryo-ET and single-molecule imaging remains an important unmet need. Experimentally, establishing a workflow that applies iSCAT or TIRF-based kinetic measurements and cryo-EM structural analysis to identical defined-isotype, defined-PTM samples in a coordinated manner represents the most direct path toward resolving these questions and forms the methodological foundation for the integrated analysis discussed in Section 6.

6. Transport sorting, physiology, disease, integrated model, and perspectives

6.1. Detyrosination as a directional routing signal for intracellular transport

It had long been assumed that the long lifetime and stability of detyrosinated microtubules reflected an intrinsic physical hardening or resistance to depolymerization. Chen et al. [16] demonstrated, however, that detyrosination does not directly alter intrinsic microtubule dynamics, neither the polymerization rate nor the depolymerization rate, but instead exerts its effects through the selective recruitment of effector proteins such as MAPs and motor proteins (kinesins and dyneins), dramatically altering their binding affinities. Detyrosination is therefore understood to function as a directional routing signal for intracellular cargo transport. Consistent with this, CLIP-170, a representative +TIP protein harboring a CAP-Gly domain, was found to bind preferentially to tyrosinated microtubules and track their plus-ends; similarly, $p150^{Glued}$, another CAP-Gly-domain protein, is excluded from detyrosinated microtubules, demonstrating that this domain recognizes the terminal tyrosine residue.

The most spatially precise illustration of code-dependent transport directionality comes from the intraflagellar transport (IFT) system. Axonemal microtubule doublets consist of A- and B-tubules; anterograde IFT trains travel along the B-tubule while retrograde trains return via the A-tubule, enabling bidirectional traffic without collision. The mechanism underlying this sorting had remained elusive until Chhatre et al. [17] focused on the differential tubulin modification states of each tubule. Using VashL-knockout *Chlamydomonas reinhardtii* mutants in which the tyrosination/detyrosination balance was disrupted, IFT train stalling was frequently observed and cilia failed to elongate normally; direct measurement revealed that anterograde and retrograde trains possess distinct affinities for A-

and B-tubules that depend on their tyrosination status.

Girão et al. [42] further showed that α-tubulin detyrosination plays a critical role in accurate chromosome segregation at the molecular level. Detyrosinated microtubules stabilize kinetochore attachment and help maintain the tension required to pull chromosomes toward the poles; when detyrosination is impaired, kinetochore–microtubule attachment errors arise, and the risk of chromosome mis-segregation increases. At the cell level, kinesin-1-mediated transport of APC to the cell cortex along detyrosinated microtubule tracks may constitute the basis of a positive feedback loop in which local microtubule stabilization reinforces further detyrosination [16]. Detyrosination-driven symmetry breaking has also been shown to control directional cell migration, underscoring the broad spatial role of the tubulin code in establishing cellular polarity [43].

6.2. Neuronal physiology: axon regeneration and neurodegeneration

Cryo-EM analysis of axonal microtubules in cortical neurons differentiated from human iPSCs revealed that, despite being GDP-bound, the lattice maintains a GTP-like expanded conformation [30]. Separately, it has been established that CNS injury induces excessive detyrosination in neurons, and that this over-modification acts as an inhibitory factor for axonal regeneration. Leibinger et al. [44] demonstrated that administration of parthenolide, which acts as an irreversible inhibitor of VASH/SVBP cysteine protease activity through alkylation of the catalytic cysteine residue, significantly promotes axonal regeneration in cultured mouse CNS neurons and human retinal ganglion cells (RGCs), indicating that modulating the tubulin code represents a promising therapeutic strategy for neural regeneration.

Tau pathology and the tubulin tyrosination cycle converge on microtubule dynamics and synaptic vulnerability in Alzheimer's disease. Peris et al. [45] found reduced tubulin tyrosine ligase (TTL) expression in sporadic and familial Alzheimer's disease, increased detyrosinated and Δ2 tubulin in patient brain, and reduced microtubule dynamics in human neurons carrying the APP-V717I mutation. In TTL-heterozygous mice, reduced tyrosination was accompanied by loss of dendritic spines, impaired synaptic plasticity, and memory deficits; conversely, restoring TTL protected dendritic spines from oligomeric amyloid-β-induced loss [45]. These findings place defective re-tyrosination upstream of a measurable synaptic phenotype and provide a direct disease link for the tyrosination/detyrosination cycle, although the extent to which this pathway interacts causally with tau aggregation remains unresolved [45,46].

Neurodegeneration can also result from dysregulation of another arm of the tubulin code, polyglutamylation. In CCP1-deficient mice, excessive tubulin polyglutamylation causes cell-autonomous neuronal degeneration and reduces the efficiency of neuronal cargo transport; deletion of the counteracting polyglutamylase TTLL1 rescues susceptible neurons [47]. The subunit specificity of this pathway is important: TTLL1-dependent α-tubulin polyglutamylation, but not TTLL7-dependent β-tubulin glutamylation, drives hyperglutamylation and degeneration in the CCP1-deficient background [20]. In humans, biallelic loss-of-function variants in CCP1/AGTPBP1 cause infantile-onset neurodegeneration affecting the cerebellum, spinal motor neurons, and peripheral nerves [48]. Together, these studies broaden the disease relevance of the tubulin code beyond detyrosination and illustrate how imbalance between PTM writers and erasers can disrupt transport and neuronal survival.

6.3. Tubulinopathies and inherited disorders of the tubulin code

Tubulinopathies provide a direct route from the genetic axis of the tubulin code to altered microtubule PTM landscapes. Jaramillo-Restrepo et al. [21] examined the taiep rat, which carries the TUBB4A A302T mutation and models hypomyelination with atrophy of the basal ganglia and cerebellum (H-ABC). White-matter regions displayed increased tubulin acetylation and detyrosination together with altered tubulin phosphorylation, and elevated acetylated tubulin was observed in oligodendrocyte-marker-positive cells. Structural modeling suggested that the A302T substitution can alter local interactions involving phosphorylated β-tubulin, consistent with increased microtubule stability [21]. Importantly, this study establishes an association rather than a direct kinetic link between the β-tubulin mutation and α-tubulin detyrosination. Whether the mutation modifies lattice conformation, microtubule lifetime, or access of detyrosinating enzymes remains to be determined. The oligodendrocyte phenotype also emphasizes that disease-causing tubulin-code dysregulation is not restricted to neurons.

Inherited defects in the detyrosination machinery provide a complementary example. Iqbal et al. [49] reported that biallelic loss-of-function mutations in SVBP cause severe intellectual disability, microcephaly, ataxia, and hypotonia, establishing an essential role for the VASH/SVBP system in neurodevelopment. Launay et al. [50] subsequently used patient-derived fibroblasts and SVBP-deficient cells to show that altered detyrosination is accompanied by centrosome-cohesion defects, impaired pericentriolar-material trafficking, mitotic abnormalities, cytokinesis failure, and premature cellular senescence, linking SVBP malfunction to a complex hereditary spastic paraplegia. Together with the TUBB4A and CCP1 disorders described above, these human genetic data illustrate that disease can arise from disruption of distinct layers of the tubulin code: The tubulin building block, a PTM-writing enzyme complex, or a PTM-erasing enzyme.

6.4. Cardiac physiology: detyrosination and heart function

In cardiomyocytes, microtubules are not merely structural scaffolds but dynamic elements that actively regulate the mechanical properties of the cell; detyrosinated microtubules support the cytoskeleton under the mechanical demands of cyclic contraction, helping to distribute stress across the cell. Under conditions of mechanical cardiac overload associated with heart failure, this balance shifts markedly toward detyrosination, and detyrosinated microtubules (dTyr-MTs) accumulate abnormally. The resulting dense, stiff MT network mechanically impedes the contraction–relaxation cycle of cardiomyocytes, contributing to disease progression [35]. Inhibition of detyrosination in human cardiomyocytes, or restoration of tyrosinated tubulin through TTL introduction, produced significant improvements in contractility and measurable reductions in stiffness in heart failure cardiomyocytes [36], suggesting that the detyrosination/re-tyrosination cycle is an essential regulator of cardiac mechanical function.

Mechanistic studies in failing human cardiomyocytes strengthen this link. Chen et al. [51] showed that failing hearts contain dense, heavily detyrosinated microtubule networks associated with increased myocyte stiffness and impaired contractility; pharmacological or genetic reduction of detyrosinated microtubules softened cardiomyocytes and restored a substantial fraction of lost contractile function. Subsequent depletion experiments identified VASH1/SVBP as a predominant cardiac detyrosinase: VASH1 knockdown reduced stiffness and accelerated contraction and relaxation in failing human

cardiomyocytes, including cells from patients with heart failure with preserved ejection fraction, without requiring altered Ca^{2+} cycling [52]. Together with the demonstration that sustained activation of tubulin tyrosination improves cardiac function [36], these findings connect the enzymatic detyrosination/re-tyrosination balance directly to tissue mechanics and identify this cycle as a potentially druggable component of cardiac disease.

6.5. Cancer and therapeutic response

Microtubule-targeting agents make cancer a particularly direct context in which tubulin-code state can influence therapeutic response. Lopes et al. [53] profiled tubulin PTM signatures across the NCI-60 cancer cell panel and found that acetylated, detyrosinated, and Δ2 α-tubulin can become uncoupled across tumor cell lines. Experimentally increasing α-tubulin detyrosination enhanced taxol cytotoxicity, in part through suppression of the detyrosination-sensitive microtubule depolymerase MCAK, thereby increasing mitotic errors and cell death [53]. Thus, detyrosination can modify the cellular response to a drug that acts by stabilizing the microtubule lattice.

However, the relationship is context dependent rather than monotonic. In ovarian cancer cells, CRISPR-mediated loss of VASH2 reduced detyrosinated tubulin yet increased paclitaxel sensitivity [54]. This apparent contrast with the MCAK-based mechanism underscores that drug response depends on the broader cellular context, including the relative abundance of VASH isoforms, TTL, depolymerizing kinesins, other PTMs, and cell-cycle state. Accordingly, tubulin PTMs may serve as biomarkers or therapeutic modifiers rather than simple universal predictors of taxane sensitivity. The dual intracellular tubulin-carboxypeptidase activity and extracellular angiogenesis-related functions of vasohibins further make this enzyme family an unusual interface between cytoskeletal regulation and tumor biology [54,55].

6.6. Integrated model: evidence for the causal cascade

In Section 3, we proposed that the tubulin code functions as a causal cascade: "isotype → lattice mechanical state → PTM enzyme accessibility → reader recruitment". We present this cascade not as an established mechanistic pathway but as a working hypothesis, a roadmap intended to organize existing evidence and prioritize experiments for the coming decade (Figure 4; Section 6.7). As detailed below, only individual fragments of this chain have been directly tested, typically two adjacent steps within a single study; no experiment to date has traced three or more consecutive steps in the same system. The subsequent sections have provided experimental support for each step of this chain. First, quantitative analysis using defined-isotype recombinant microtubules demonstrated that isotype composition directly changes microtubule growth and catastrophe behavior and is associated with differences in plus-end taper and tubulin curvature [3], while the expanded-to-compacted conformational transition of the lattice was visualized at atomic resolution [2]. Second, MD simulations and live-cell biosensor experiments established that lattice expansion shifts the α-tubulin CTT from a "stored" to an "accessible" state [11], and that the catalytic activity, but not the binding of VASH1/SVBP, is specifically enhanced on expanded lattices [9]. How this conformation-dependent activity regulation is integrated with the stochastic stability-dependent feedback loop proposed by Tang et al. [31] remains unresolved, and mechanistic understanding of this step is developing. Third, A/B-tubule sorting of IFT trains [17] and kinesin-1-mediated APC transport [16] constitute the most direct

experimental evidence that specific PTM patterns recruit specific effectors. Nevertheless, no single experimental system has demonstrated this causal cascade in its entirety; the connections between individual steps remain inferential, and their complete experimental validation is the central challenge addressed in the following section.

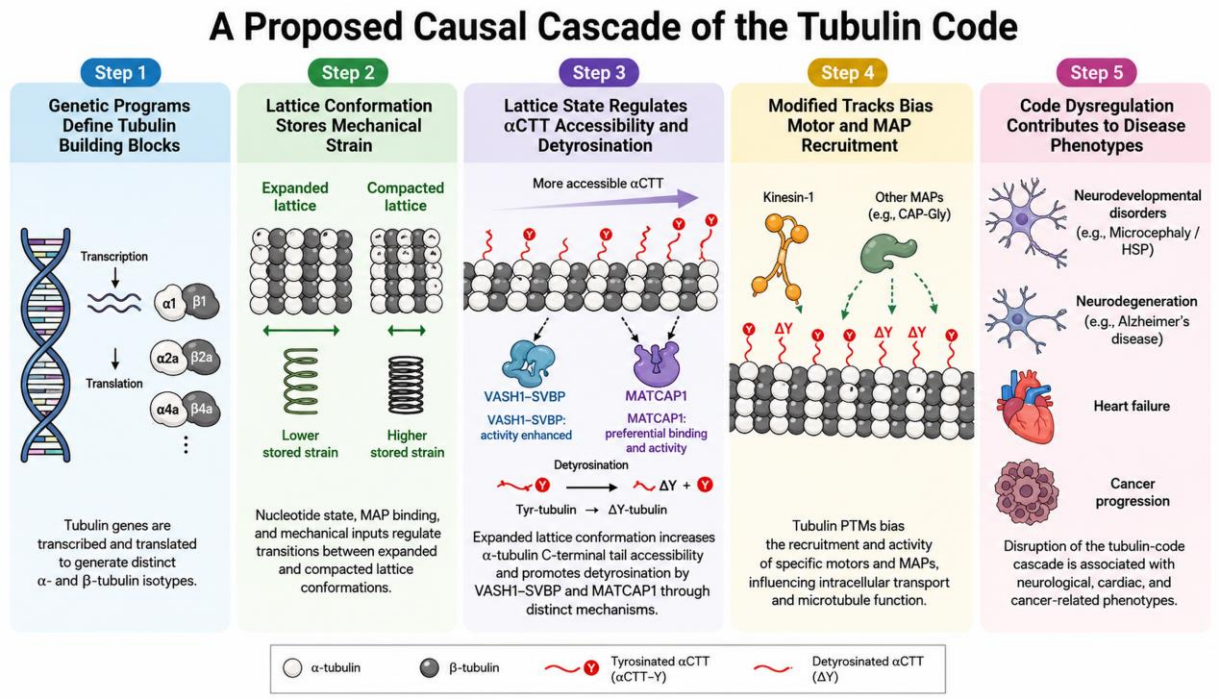

Figure 4. A proposed five-step causal cascade linking tubulin genetics to disease phenotypes.

Integrated summary of the causal chain proposed throughout this review (Section 6.6). Step 1: Transcription and translation of distinct tubulin genes generate the α- and β-tubulin isotype repertoire (Section 3.2) [3]. Step 2: Nucleotide state, MAP binding, and mechanical inputs drive transitions between expanded (lower stored strain) and compacted (higher stored strain) lattice conformations (Section 5.1) [2]. Step 3: Lattice expansion increases α-tubulin CTT accessibility and promotes detyrosination, enhancing VASH1/SVBP catalytic activity and the binding and activity of MATCAP through distinct mechanisms (Section 4.4) [9,11,29]. Step 4: The resulting tubulin PTM patterns bias the recruitment and activity of specific motors (e.g., kinesin-1) and MAPs (e.g., CAP-Gly domain proteins), shaping intracellular transport and microtubule function (Section 6.1) [16,17]. Step 5: Disruption of this cascade is associated with neurodevelopmental and hereditary motor-neuron disorders (e.g., microcephaly, hereditary spastic paraplegia), neurodegeneration (e.g., Alzheimer's disease), heart failure, and cancer progression (Section 6.2–6.5) [21,45,49–55]. As emphasized in the main text, each individual link in this cascade is supported by independent experimental evidence, but no single study has traced the complete chain within one integrated system (Section 6.6). Arrows in this diagram therefore denote proposed, not experimentally proven, causal links; the Step 2→3 link (quantitatively coupling lattice mechanics to enzyme kinetics in one system) and the Step 4→5 link (tracing specific PTM-effector events causally to organismal phenotypes) are the weakest-supported and most speculative transitions in the cascade.

6.7. Future experimental priorities and concluding remarks

To resolve the open questions identified throughout this review, the following experimental approaches represent the most critical priorities. First, while biosensors capture CTT exposure, the development of a complementary "lattice-state sensor" capable of reporting the expanded versus compacted conformation in real time, combined with in situ cryo-ET of cells under defined stimuli to directly visualize the local lattice state alongside bound PTM enzymes and motor proteins at atomic resolution, would close the most fundamental observational gap. Second, integrating the stochastic enzyme kinetics and stability feedback loop proposed by Tang et al. [31] will require optogenetic probes that enable light-controlled manipulation of enzyme activity with millisecond temporal resolution, together with multi-color PTM imaging to track the precise timing and position of enzyme recruitment to the lattice. Third, an in vitro reconstitution system that polymerizes microtubules of defined isotype composition, introduces PTM enzymes, and continuously quantifies the resulting modification state together with downstream effector recruitment in a single integrated pipeline would provide the most direct test of the integrated tubulin code model. Fourth, CRISPR/Cas9-based genetic strategies that introduce disease-relevant isotype compositions or PTM enzyme activities into normal cells, and then monitor which step in the code cascade fails, would localize the points of breakdown in pathological contexts and generate actionable therapeutic targets.

Microtubules are not merely a passive cytoskeletal scaffold; they constitute a biological information processing system in which isotype composition, lattice mechanical properties, and an elaborate repertoire of post-translational modifications are integrated with precision. As this review has illustrated, the convergence of structural biology and quantitative biochemical approaches is progressively revealing the depth to which the tubulin code governs cell fate and function. Demonstrating this multi-layered integration in a single, unified experimental system will stand as the central challenge of microtubule biology in the coming decade.

Use of generative-AI tools declaration

During the preparation and revision of this manuscript, the authors used ChatGPT (OpenAI), NotebookLM (Google) and Claude (Anthropic) to assist with literature organization, language editing, manuscript revision, and the conceptual development and refinement of schematic figures. All AI-assisted outputs were critically reviewed, verified against primary sources where applicable, and edited by the authors. The authors take full responsibility for the accuracy and integrity of the final manuscript.

Acknowledgments

The literature on the tubulin code has grown rapidly in recent years, and despite our efforts to provide a comprehensive synthesis, space and scope constraints prevented us from citing many additional valuable studies relevant to this field. We apologize to the authors of those works and thank the broader research community for their contributions.

This work was supported by the Japan Society for the Promotion of Science (JSPS) KAKENHI Grant Number 23K05671.

Conflict of interest

All authors declare no conflicts of interest in this paper.

Author contributions

Conceptualization, supervision, and project administration: T.N.; Investigation, literature review, and writing – original draft: M.H.; Writing – review and editing: S.I. and T.N. All authors have read and approved the final version of the manuscript for publication.

References

1. Brouhard GJ, Rice LM (2018) Microtubule dynamics: an interplay of biochemistry and mechanics. *Nat Rev Mol Cell Biol* 19: 451–463. https://doi.org/10.1038/s41580-018-0009-y
2. Alushin GM, Lander GC, Kellogg EH, et al. (2014) High-resolution microtubule structures reveal the structural transitions in αβ-tubulin upon GTP hydrolysis. *Cell* 157: 1117–1129. https://doi.org/10.1016/j.cell.2014.03.053
3. Vemu A, Atherton J, Spector JO, et al. (2017) Tubulin isoform composition tunes microtubule dynamics. *Mol Biol Cell* 28: 3564–3572. https://doi.org/10.1091/mbc.E17-02-0124
4. Aillaud C, Bosc C, Peris L, et al. (2017) Vasohibins/SVBP are tubulin carboxypeptidases (TCPs) that regulate neuron differentiation. *Science* 358: 1448–1453. https://doi.org/10.1126/science.aao4165
5. Nieuwenhuis J, Adamopoulos A, Bleijerveld OB, et al. (2017) Vasohibins encode tubulin detyrosinating activity. *Science* 358: 1453–1456. https://doi.org/10.1126/science.aao5676
6. Roll-Mecak A (2020) The tubulin code in microtubule dynamics and information encoding. *Dev Cell* 54: 7–20. https://doi.org/10.1016/j.devcel.2020.06.008
7. Janke C, Magiera MM (2020) The tubulin code and its role in controlling microtubule properties and functions. *Nat Rev Mol Cell Biol* 21: 307–326. https://doi.org/10.1038/s41580-020-0214-3
8. McKenna ED, Sarbanes SL, Cummings SW, et al. (2023) The tubulin code, from molecules to health and disease. *Annu Rev Cell Dev Biol* 39: 331–361. https://doi.org/10.1146/annurev-cellbio-030123-032748
9. Yue Y, Hotta T, Higaki T, et al. (2023) Microtubule detyrosination by VASH1: SVBP is regulated by the conformational state of tubulin in the lattice. *Curr Biol* 33: 4111–4123.e7. https://doi.org/10.1016/j.cub.2023.07.062
10. Li F, Li Y, Ye X, et al. (2020) Cryo-EM structure of VASH1-SVBP bound to microtubules. *eLife* 9: e58157. https://doi.org/10.7554/eLife.58157
11. Hotta T, Pimm ML, Thomas EC, et al. (2026) Accessibility of the unstructured α-tubulin C-terminal tail is controlled by microtubule lattice conformation. *eLife* 14: RP109308. https://doi.org/10.7554/eLife.109308.3
12. Vemu A, Atherton J, Spector JO, et al. (2016) Structure and dynamics of single-isoform recombinant neuronal human tubulin. *J Biol Chem* 291: 12907–12915. https://doi.org/10.1074/jbc.C116.731133

13. Ramirez-Rios S, Liao S, Dumont E, et al. (2023) VASH1-SVBP and VASH2-SVBP generate different detyrosination profiles on microtubules. *J Cell Biol* 222: e202205096. https://doi.org/10.1083/jcb.202205096
14. Kalutskii M, Grubmüller H, Volkov VA, et al. (2025) Microtubule dynamics are defined by conformations and stability of clustered protofilaments. *Proc Natl Acad Sci USA* 122: e2424263122. https://doi.org/10.1073/pnas.2424263122
15. Colonna G (2025) Protein biophysics: current limitations and prospects. *AIMS Biophys* 12: 333–374. https://doi.org/10.3934/biophy.2025018
16. Chen J, Kholina E, Szyk A, et al. (2021) α-tubulin tail modifications regulate microtubule stability through selective effector recruitment, not changes in intrinsic polymer dynamics. *Dev Cell* 56: 2016–2028.e4. https://doi.org/10.1016/j.devcel.2021.05.005
17. Chhatre A, Stepanek L, Nievergelt AP, et al. (2025) Tubulin tyrosination/detyrosination regulate the affinity and sorting of intraflagellar transport trains on axonemal microtubule doublets. *Nat Commun* 16: 1055. https://doi.org/10.1038/s41467-025-56098-0
18. Janke C, Rogowski K, Wloga D, et al. (2005) Tubulin polyglutamylase enzymes are members of the TTL domain protein family. *Science* 308: 1758–1762. https://doi.org/10.1126/science.1113010
19. Lacroix B, van Dijk J, Gold ND, et al. (2010) Tubulin polyglutamylation stimulates spastin-mediated microtubule severing. *J Cell Biol* 189: 945–954. https://doi.org/10.1083/jcb.201001024
20. Bodakuntla S, Yuan X, Genova M, et al. (2021) Distinct roles of α- and β-tubulin polyglutamylation in controlling axonal transport and in neurodegeneration. *EMBO J* 40: e108498. https://doi.org/10.15252/embj.2021108498
21. Jaramillo-Restrepo C, Piazza V, Hernandez-Morales I, et al. (2026) H-ABC tubulinopathy exhibits a cytoskeletal defect associated with microtubule stability. *Neurobiol Dis* 224: 107420. https://doi.org/10.1016/j.nbd.2026.107420
22. Watanabe K, Hasegawa Y, Yamashita H, et al. (2004) Vasohibin as an endothelium-derived negative feedback regulator of angiogenesis. *J Clin Invest* 114: 898–907. https://doi.org/10.1172/JCI21152
23. Sato Y, Sonoda H (2007) The vasohibin family: a negative regulatory system of angiogenesis genetically programmed in endothelial cells. *Arterioscler Thromb Vasc Biol* 27: 37–41. https://doi.org/10.1161/01.ATV.0000252062.48280.61
24. Du H, Zhao J, Hai L, et al. (2017) The roles of vasohibin and its family members: beyond angiogenesis modulators. *Cancer Biol Ther* 18: 827–832. https://doi.org/10.1080/15384047.2017.1373217
25. Liao S, Rajendraprasad G, Wang N, et al. (2019) Molecular basis of vasohibins-mediated detyrosination and its impact on spindle function and mitosis. *Cell Res* 29: 533–547. https://doi.org/10.1038/s41422-019-0187-y
26. Wang N, Bosc C, Choi SR, et al. (2019) Structural basis of tubulin detyrosination by the vasohibin–SVBP enzyme complex. *Nat Struct Mol Biol* 26: 571–582. https://doi.org/10.1038/s41594-019-0241-y
27. Zhou C, Bhatt TK, Bharat TAM, et al. (2019) Structural basis of tubulin detyrosination by VASH2/SVBP heterodimer. *Nat Commun* 10: 3212. https://doi.org/10.1038/s41467-019-11277-8

28. Ikeda A, Urata S, Ando T, et al. (2020) The crystal structure of the tetrameric human vasohibin-1–SVBP complex reveals a variable arm region within the structural core. *Acta Crystallogr D Struct Biol* 76: 993–1000. https://doi.org/10.1107/S2059798320011298
29. Yue Y, Hotta T, Ohi R, et al. (2026) MATCAP1 preferentially binds an expanded tubulin conformation to generate detyrosinated and ΔC2 α-tubulin. *EMBO J* 45: 4257–4282. https://doi.org/10.1038/s44318-026-00772-6
30. Zehr EA, Sun S, Sarbanes SL, et al. (2026) Microtubules in the axon are GDP bound but adopt a stable GTP-like expanded state. *Nat Struct Mol Biol* 33: 631–640. https://doi.org/10.1038/s41594-026-01787-7
31. Tang Q, Sangha AK, Bharat TAM, et al. (2023) Interplay between stochastic enzyme activity and microtubule stability drives detyrosination enrichment on microtubule subsets. *Curr Biol* 33: 5334–5347. https://doi.org/10.1016/j.cub.2023.10.068
32. Landskron L, Bak J, Adamopoulos A, et al. (2022) Posttranslational modification of microtubules by the MATCAP detyrosinase. *Science* 376: eabn6020. https://doi.org/10.1126/science.abn6020
33. Nicot S, Gillard G, Impheng H, et al. (2023) A family of carboxypeptidases catalyzing α- and β-tubulin tail processing and deglutamylation. *Sci Adv* 9: eadi7838. https://doi.org/10.1126/sciadv.adi7838
34. Simon M, Espeut J, Juge F, et al. (2025) Real-time FRET assay for monitoring detyrosination by TMCP1 and VASH2. *Protein Sci* 34: e70374. https://doi.org/10.1002/pro.70374
35. Sanyal C, Pietsch N, Ramirez Rios S, et al. (2023) The detyrosination/re-tyrosination cycle of tubulin and its role and dysfunction in neurons and cardiomyocytes. *Semin Cell Dev Biol* 137: 46–62. https://doi.org/10.1016/j.semcdb.2021.12.006
36. Pietsch N, Chen CY, Kupsch S, et al. (2024) Chronic activation of tubulin tyrosination improves heart function. *Circ Res* 135: 910–932. https://doi.org/10.1161/CIRCRESAHA.124.324387
37. Chew YM, Cross RA (2025) Structural switching of tubulin in the microtubule lattice. *Biochem Soc Trans* 53: 161–171. https://doi.org/10.1042/BST20240360
38. Cleary JM, Kim T, Cook ASI, et al. (2022) Measurements and simulations of microtubule growth imply strong longitudinal interactions and reveal a role for GDP on the elongating end. *eLife* 11: e75931. https://doi.org/10.7554/eLife.75931
39. Estévez-Gallego J, Blum TB, Ruhnow F, et al. (2025) Hydrolysis-deficient mosaic microtubules as faithful mimics of the GTP cap. *Nat Commun* 16: 2396. https://doi.org/10.1038/s41467-025-57555-6
40. Zhou J, Wang A, Song Y, et al. (2023) Structural insights into the mechanism of GTP initiation of microtubule assembly. *Nat Commun* 14: 5980. https://doi.org/10.1038/s41467-023-41615-w
41. de Jager L, Jansen KI, Hoogebeen R, et al. (2025) StableMARK-decorated microtubules in cells have expanded lattices. *J Cell Biol* 224: e202206143. https://doi.org/10.1083/jcb.202206143
42. Girão H, Macário-Monteiro J, Figueiredo AC, et al. (2024) α-tubulin detyrosination fine-tunes kinetochore-microtubule attachments. *Nat Commun* 15: 9720. https://doi.org/10.1038/s41467-024-54155-8
43. Lavrsen K, Rajendraprasad G, Leda M, et al. (2023) Microtubule detyrosination drives symmetry breaking to polarize cells for directed cell migration. *Proc Natl Acad Sci USA* 120: e2300322120. https://doi.org/10.1073/pnas.2300322120

44. Leibinger M, Zeitler C, Paulat M, et al. (2023) Inhibition of microtubule detyrosination by parthenolide facilitates functional CNS axon regeneration. *eLife* 12: e88279. https://doi.org/10.7554/eLife.88279
45. Peris L, Parato J, Qu X, et al. (2022) Tubulin tyrosination regulates synaptic function and is disrupted in Alzheimer's disease. *Brain* 145: 2486–2506. https://doi.org/10.1093/brain/awab436
46. Chu D, Liu F (2019) Pathological changes of tau related to Alzheimer's disease. *ACS Chem Neurosci* 10: 931–944. https://doi.org/10.1021/acschemneuro.8b00457
47. Magiera MM, Bodakuntla S, Žiak J, et al. (2018) Excessive tubulin polyglutamylation causes neurodegeneration and perturbs neuronal transport. *EMBO J* 37: e100440. https://doi.org/10.15252/embj.2018100440
48. Shashi V, Magiera MM, Klein D, et al. (2018) Loss of tubulin deglutamylase CCP1 causes infantile-onset neurodegeneration. *EMBO J* 37: e100540. https://doi.org/10.15252/embj.2018100540
49. Iqbal Z, Tawamie H, Ba W, et al. (2019) Loss of function of SVBP leads to autosomal recessive intellectual disability, microcephaly, ataxia, and hypotonia. *Genet Med* 21: 1790–1796. https://doi.org/10.1038/s41436-018-0415-8
50. Launay N, Espinosa-Alcantud M, Verdura E, et al. (2025) Altered tubulin detyrosination due to SVBP malfunction induces cytokinesis failure and senescence, underlying a complex hereditary spastic paraplegia. *Aging Cell* 24: e14355. https://doi.org/10.1111/acel.14355
51. Chen CY, Caporizzo MA, Bedi K, et al. (2018) Suppression of detyrosinated microtubules improves cardiomyocyte function in human heart failure. *Nat Med* 24: 1225–1233. https://doi.org/10.1038/s41591-018-0046-2
52. Chen CY, Salomon AK, Caporizzo MA, et al. (2020) Depletion of vasohibin 1 speeds contraction and relaxation in failing human cardiomyocytes. *Circ Res* 127: e14–e27. https://doi.org/10.1161/CIRCRESAHA.119.315947
53. Lopes D, Seabra AL, Orr B, et al. (2023) α-Tubulin detyrosination links the suppression of MCAK activity with taxol cytotoxicity. *J Cell Biol* 222: e202205092. https://doi.org/10.1083/jcb.202205092
54. Koyanagi T, Saga Y, Takahashi Y, et al. (2021) Knockout of vasohibin-2 reduces tubulin carboxypeptidase activity and increases paclitaxel sensitivity in ovarian cancer. *Cancer Med* 10: 2732–2739. https://doi.org/10.1002/cam4.3841
55. Abbas G, Kirabo A, Ahmed U, et al. (2025) Vasohibins in health and disease: from angiogenesis to tumorigenesis, multiorgan dysfunction, and brain-heart remodeling. *Cells* 14: 767. https://doi.org/10.3390/cells14110767

AIMS Press